Supplementary Information

Hybriding Fe_3O_4 nanocrystals with nitrogen-doped carbon nanowires for high-performance supercapacitors †

Jizhang Chen,*[a] Qiongyu Chen,[a] Junling Xu[b] and Ching-Ping Wong[b]

[a.] *College of Materials Science and Engineering, Nanjing Forestry University, Nanjing 210037, China.*
[b.] *Department of Electronic Engineering, The Chinese University of Hong Kong, New Territories, Hong Kong.*

E-mail address: jizhang.chen@hotmail.com (J. Chen).

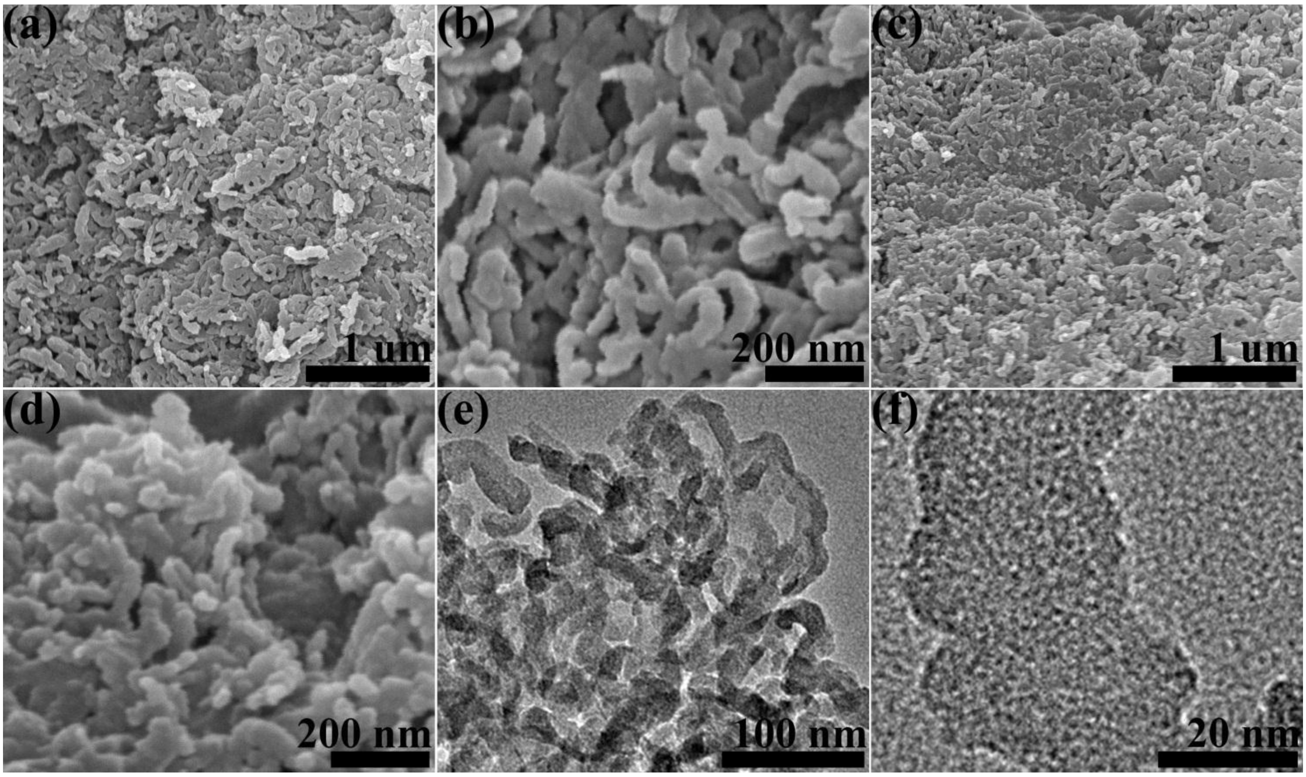

Fig. S1 SEM and TEM images of (a, b) PPy nanowires and (c–f) NCN.

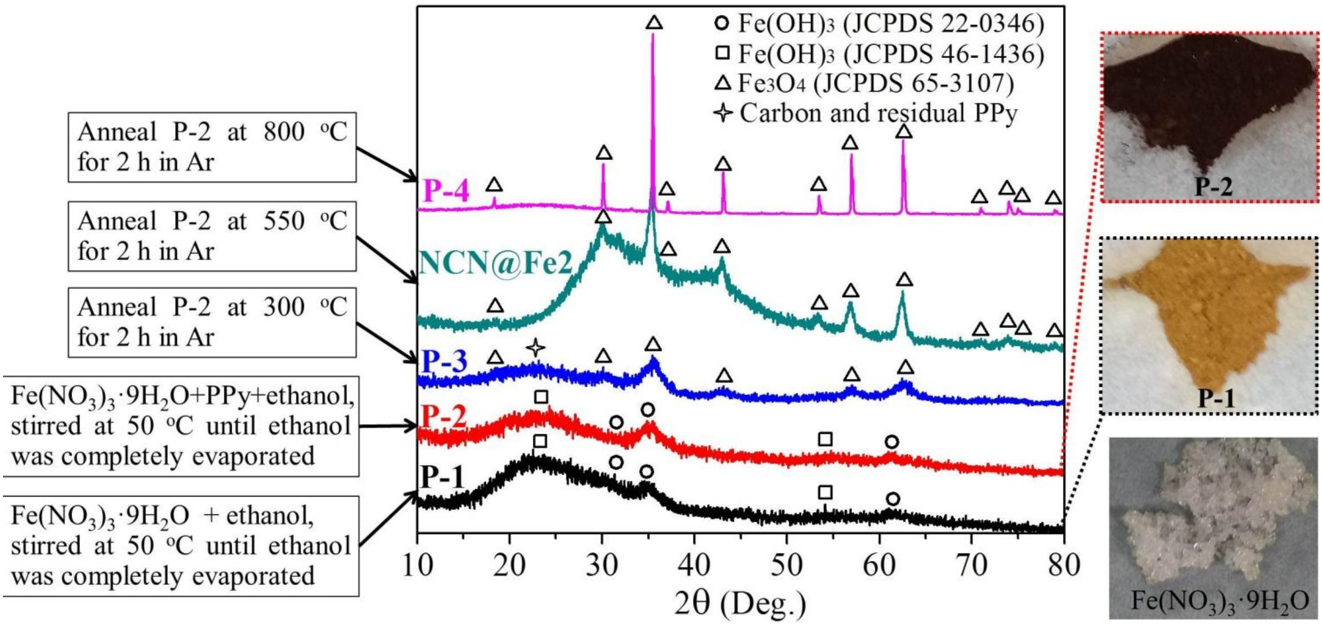

Fig. S2 XRD patterns of different products when altering the raw material or annealing temperature.

P-1 is obtained without the addition of PPy. From the XRD pattern of P-1 and the photographs (on the right of XRD patterns), we can see that the $Fe(NO_3)_3$ $9H_2O$ precursor was hydrolyzed to $Fe(OH)_3$ after dissolved in ethanol and subsequently evaporating ethanol at 50 ^oC. When PPy was added, the product P-2 exhibits nearly the same XRD pattern as that of P-1. The signal from PPy is so weak that it is covered up by that of $Fe(OH)_3$. After annealing P-2 at 300 ^oC for 2 h in Ar atmosphere, P-3 was obtained. Except for a hump arising from carbon and residual PPy, all the peaks of P-3 can be indexed to Fe_3O_4 (JCPDS 65-3107). When the annealing temperature was increased to 550 ^oC, the obtained NCN@Fe2 keeps the Fe_3O_4 phase and its crystallinity is much higher than that of P-3. When the annealing temperature was further increased to 800 ^oC, the obtained P-4 shows sharp peaks of Fe_3O_4, indicative of large particle size and rather high crystallinity.

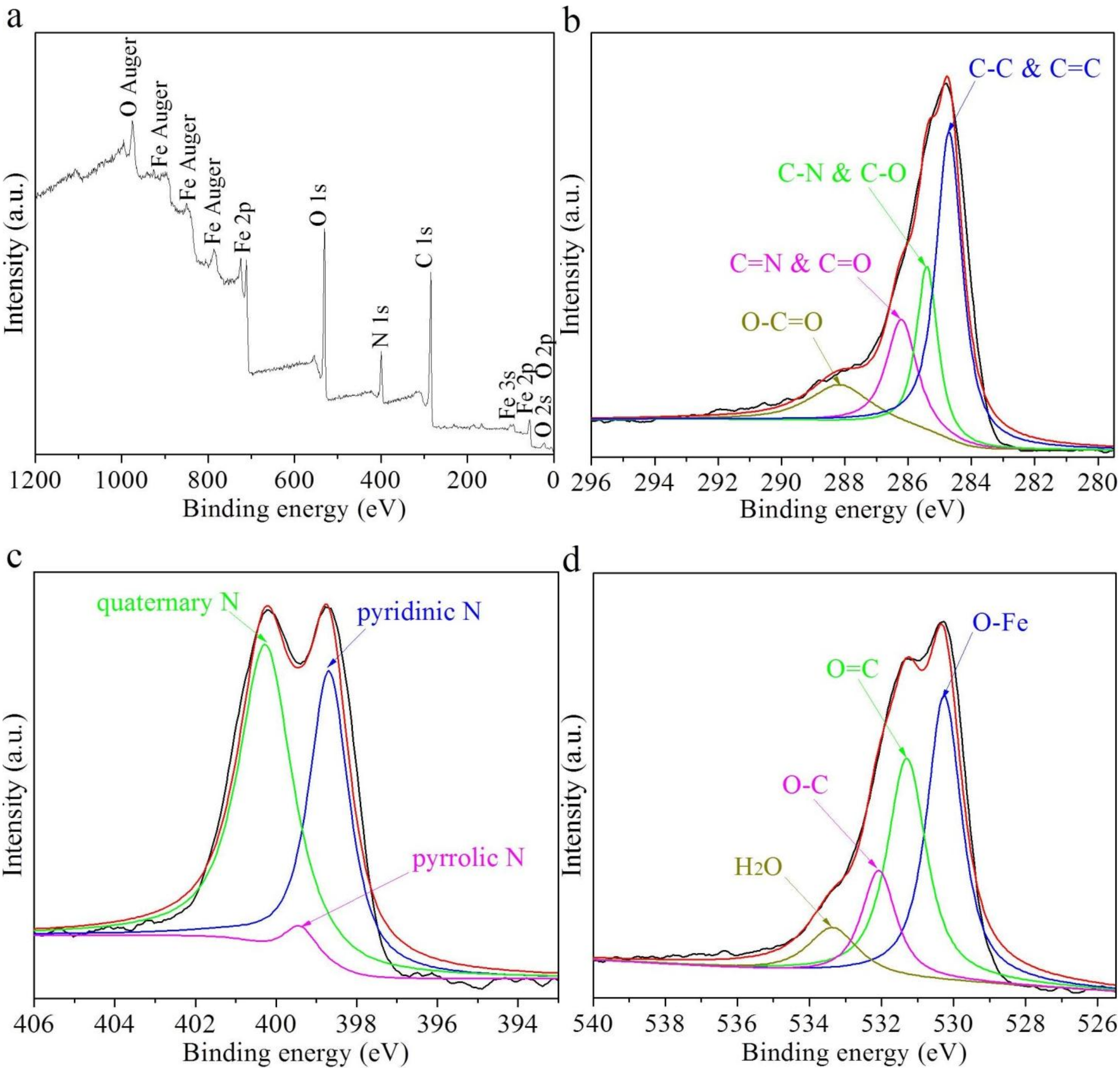

Fig. S3 (a) Survey XPS spectrum and (b) C 1s, (c) N 1s, and (d) O 1s HR XPS spectra of NCN@Fe2.

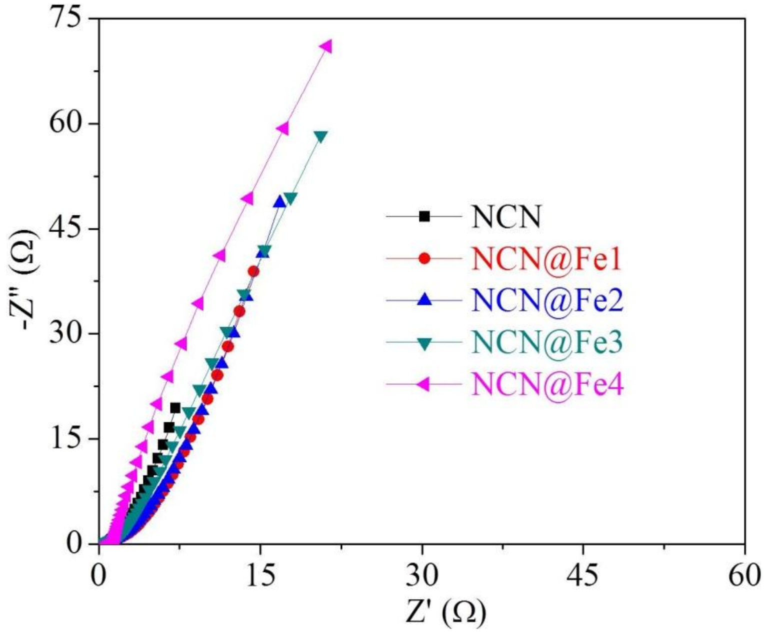

Fig. S4 Nyquist plots of NCN, NCN@Fe1, NCN@Fe2, NCN@Fe3, and NCN@Fe4.

Table S1 Specific capacitance of NCN@Fe2 versus Fe-based pseudocapacitive materials reported in recent three years, all tested in 3-electrode setups.

Active material	Electrolyte	Capacitance	Ref. (Year)
NCN@Fe2	3 M KOH	541.7 F g^{-1} at 1 A g^{-1}	This work
Ti-doped Fe_2O_3@PEDOT	5 M LiCl	311.6 F g^{-1} at 1 mA cm^{-2}	[1] (2015)
graphene/Fe_2O_3 QDs	1 M Na_2SO_4	347 F g^{-1} at 10 mV s^{-1}	[2] (2015)
α-Fe_2O_3 hollow tubes	6 M KOH	330 F g^{-1} at 0.5 A g^{-1}	[3] (2016)
FeOOH/Ag/ZnO nanorods	0.5 M Li_2SO_4	376.6 F g^{-1} at 1 A g^{-1}	[4] (2016)
hollow and porous Fe_2O_3	0.5 M Na_2SO_3	346 F g^{-1} at 2 mV s^{-1}	[5] (2016)
Fe_2O_3 nanotubes	1 M Li_2SO_4	300.1 F g^{-1} at 0.75 A g^{-1}	[6] (2016)
VACNTs@Fe_2O_3	2 M KOH	248 F g^{-1} at 8 A g^{-1}	[7] (2016)
Fe_2O_3@N-doped graphene	2 M KOH	274 F g^{-1} at 1 A g^{-1}	[8] (2016)
graphene/FeOOH QDs	1 M Li_2SO_4	365 F g^{-1} at 10 mV s^{-1}	[9] (2016)
rGO/Fe_3O_4 nanoparticles	1 M KOH	241 F g^{-1} at 1 A g^{-1}	[10] (2016)
rGO/Fe_2O_3 nanotubes	1 M Na_2SO_4	262.2 F g^{-1} at 1 A g^{-1}	[11] (2017)
Fe_2O_3@C-rGO	1 M Na_2SO_4	211.4 F g^{-1} at 0.5 A g^{-1}	[12] (2017)
Fe_3O_4@hollow graphite	4 M KOH	481 F g^{-1} at 1 A g^{-1}	[13] (2017)
rGO/Fe_3O_4 nanoparticles	2 M KOH	455 F g^{-1} at 8 mV s^{-1}	[14] (2017)
Fe_2O_3@MnO_2 nanotubes	3 M KOH	289.9 F g^{-1} at 1 A g^{-1}	[15] (2017)
Fe_2O_3 nanorods	2 M KOH	516.7 F g^{-1} at 1 A g^{-1}	[16] (2017)
NiNTAs@Fe_2O_3 nanoneedles	1 M Na_2SO_4	418.7 F g^{-1} at 10 mV s^{-1}	[17] (2017)

References

1 Y. Zeng, Y. Han, Y. Zhao, Y. Zeng, M. Yu, Y. Liu, H. Tang, Y. Tong and X. Lu, *Adv. Energy Mater.*, 2015, **5**, 1402176.

2 H. Xia, C. Hong, B. Li, B. Zhao, Z. Lin, M. Zheng, S. V. Savilov and S. M. Aldoshin, *Adv. Funct. Mater.*, 2015, **25**, 627-635.

3 J. Li, W. Zhang, G. Zan and Q. Wu, *Dalton T.*, 2016, **45**, 12790-12799.

4 S. Yang, Y. Li, T. Xu, Y. Li, H. Fu, K. Cheng, K. Ye, L. Yang, D. Cao and G. Wang, *RSC Adv.*, 2016, **6**, 39166-39171.

5 C. Fu, A. Mahadevegowda and P. S. Grant, *J. Mater. Chem. A*, 2016, **4**, 2597-2604.

6 Y.-G. Lin, Y.-K. Hsu, Y.-C. Lin and Y.-C. Chen, *Electrochimica. Acta*, 2016, **216**, 287-294.

7 W. Zhang, B. Zhao, Y. Yin, T. Yin, J. Cheng, K. Zhan, Y. Yan, J. Yang and J. Li, *J. Mater. Chem. A*, 2016, **4**, 19026-19036.

8 L. Liu, J. Lang, P. Zhang, B. Hu and X. Yan, *ACS Appl. Mater. Interf.*, 2016, **8**, 9335-9344.

9 J. Liu, M. Zheng, X. Shi, H. Zeng and H. Xia, *Adv. Funct. Mater.*, 2016, **26**, 919-930.

10 L. Li, P. Gao, S. Gai, F. He, Y. Chen, M. Zhang and P. Yang, *Electrochim. Acta*, 2016, **190**, 566-573.

11 D. M. G. T. Nathan and S. J. M. Boby, *J. Alloys Compd.*, 2017, **700**, 67-74.

12 M. Zhang, J. Sha, X. Miao, E. Liu, C. Shi, J. Li, C. He, Q. Li and N. Zhao, *J. Alloys Compd.*, 2017, **696**, 956-963.

13 H. Khani and D. O. Wipf, *ACS Appl. Mater. Interf.*, 2017, **9**, 6967-6978.

14 R. Kumar, R. K. Singh, A. R. Vaz, R. Savu and S. A. Moshkalev, *ACS Appl. Mater. Interf.*, 2017, **9**, 8880-8890.

15 G. Nie, X. Lu, M. Chi, Y. Zhu, Z. Yang, N. Song and C. Wang, *Electrochim. Acta*, 2017, **231**, 36-43.

16 J. Wang, L. Zhang, X. Liu, X. Zhang, Y. Tian, X. Liu, J. Zhao and Y. Li, *Sci. Rep.*, 2017, **7**, 41088.

17 Y. Li, J. Xu, T. Feng, Q. Yao, J. Xie and H. Xia, *Adv. Funct. Mater.*, 2017, **27**, 1606728.